IEEE Access
Multidisciplinary ⋮ Rapid Review ⋮ Open Access Journal

Received 7 June 2024, accepted 28 June 2024, date of publication 2 July 2024, date of current version 23 July 2024.

Digital Object Identifier 10.1109/ACCESS.2024.3422182

RESEARCH ARTICLE

Enhancing Performance of Massive MU-MIMO System With LR-RTS: A Low-Complexity Detection Algorithm

KALAPRAVEEN BAGADI[1], (Senior Member, IEEE), VISALAKSHI ANNEPU[2], NAGA RAJU CHALLA[3], FRANCESCO BENEDETTO[4], (Senior Member, IEEE), THOKOZANI SHONGWE[5], (Senior Member, IEEE), AND KHALED RABIE[5,6], (Senior Member, IEEE)

[1]School of Electronics Engineering, VIT-AP University, Amaravati 522237, India
[2]School of Computer Science and Engineering, VIT-AP University, Amaravati 522237, India
[3]Department of ECE, Bapatla Engineering College, Bapatla 522102, India
[4]SP4TE–Signal Processing for Telecommunications and Economics Laboratory, Economics Department, University of Roma Tre, 00145 Rome, Italy
[5]Electrical and Electronic Engineering Technology, University of Johannesburg, Johannesburg 2006, South Africa
[6]Department of Engineering, Manchester Metropolitan University (MMU), M15 6BH Manchester, U.K.

Corresponding authors: Khaled Rabie (k.rabie@mmu.ac.uk) and Naga Raju Challa (nagaraju.challa@becbapatla.ac.in)

ABSTRACT In recent years, the deployment of massive multiuser multiple-input multiple-output (MU-MIMO) systems with hundreds or even thousands of antennas at the enhanced-mobile broadband station (e-MBBS) has gained considerable attention in the research community and industry for emerging applications such as millimeter-wave (mm-wave) communications, 5G and Beyond, Beamforming and spatial division multiple access (SDMA) and IoT and Wearable Devices. In this paper, we propose a novel low-complexity detection algorithm, namely lattice reduction associated reactive Tabu search (LR-RTS), capable of providing near-optimal detection performances by mitigating both the inter-antenna interference (IAI) and multi-user interference (MUI). The lattice reduction (LR)-based precoding scheme is first incorporated by the mobile user to suppress the IAI. Then, the novel LR-associated RTS detection algorithm is used at the e-MBBS to mitigate the MUI. The initial signal vector of this algorithm is chosen from the solution of the LR pre-coded ZF detector. Simulation results and comparisons with state-of-the-art methods show that the proposed solution outperforms heuristic search-based algorithms, namely likelihood ascent search (LAS) and linear detection methods like zero-forcing (ZF). In addition, our method offers a better tradeoff between performance and computational complexity for systems with a massive number of antennas and higher-order QAM modulations, showing a performance gain between 2dB and 9dB versus the conventional techniques.

INDEX TERMS Enhanced mobile broadband station, inter-antenna interference, lattice reduction, multi-user multiple input multiple output, multi-user interference, reactive-Tabu search.

I. INTRODUCTION

Massive multiple-input and multiple-output (MIMO) technology has brought forth a new era of possibilities and challenges in the rapidly evolving landscape of wireless communication. This cutting-edge technology, characterized by deploying many antennas at both the transmitter and receiver ends, holds immense potential for revolutionizing how we experience wireless connectivity [1]. Massive MIMO has become a foundation of modern wireless communication standards by significantly improving link reliability, throughput, channel capacity, and spectral efficiency without additional spectrum resources [2]. MIMO technology plays a pivotal role in enhancing link reliability and throughput with its multiple antennas. It achieves this by increasing channel capacity and spectral efficiency without requiring additional

The associate editor coordinating the review of this manuscript and approving it for publication was Zihuai Lin.

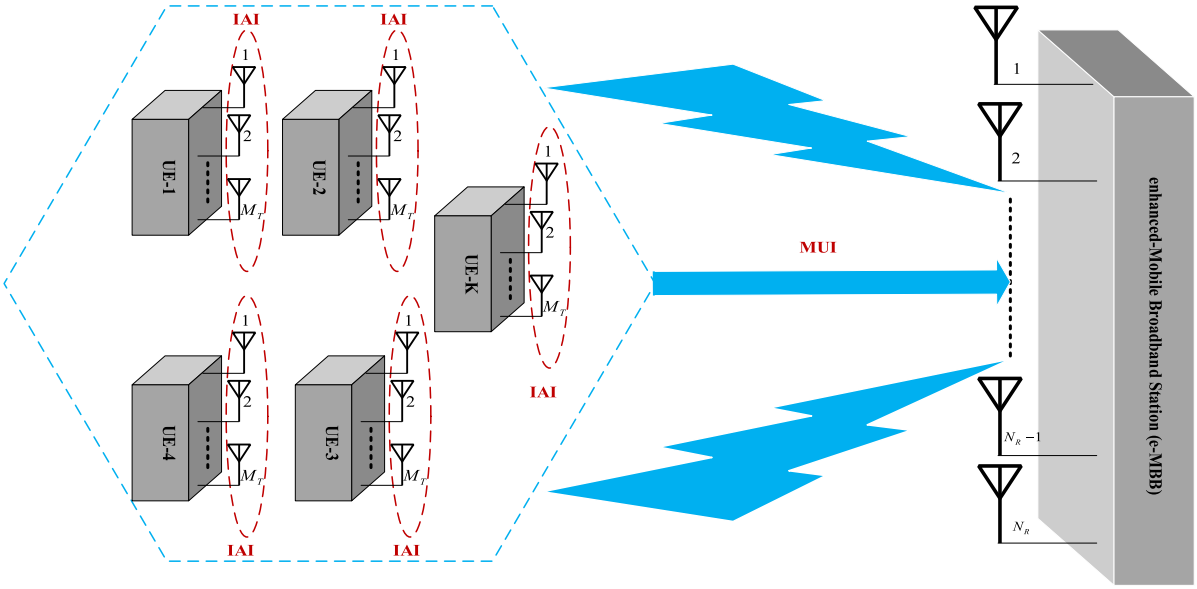

FIGURE 1. Representation of IAI and MUI.

spectrum resources [3], [4]. As a result, MIMO technology has become integral to wireless communication standards, including IEEE 802.11n (Wi-Fi) [5], IEEE 802.11ac (Wi-Fi) [6], high-speed packet access plus (HSPA+) [7], long-term evolution (LTE) (4G) [8], and LTE-advanced [9].

The large-scale multi-user MIMO (MU-MIMO) paradigm, commonly known as massive MIMO, represents a significant advancement in wireless communication technology. It is worth noting that when a MIMO system is equipped with a considerable number of antennas, it is often termed an extremely large-scale MIMO (XL-MIMO) [10] or ultra-massive MIMO (UM-MIMO) [11]. However, in practical terms, a base station (BS) with hundreds of antennas is typically referred to as a massive MIMO [12]. Realizing the full potential of Massive MIMO, particularly in large-scale MU-MIMO systems, presents significant challenges. This paper explores the critical issues affecting such systems' performance-complexity trade-offs. These challenges encompass mitigating IAI, managing MUI, accurate estimation of channel state information (CSI) for numerous channels, synchronization, and hardware implementation. Among these challenges, IAI and MUI, as depicted in Fig. 1, are critical obstacles that significantly constrain the performance of large-scale MU-MIMO systems. The primary objective of this research paper is to address these issues by introducing a novel low-complexity detection algorithm, lattice reduction associated reactive Tabu search (LR-RTS). By effectively mitigating IAI and MUI, this algorithm enhances the performance of large-scale MU-MIMO systems, thus unlocking the full potential of massive MIMO in future wireless communication.

This paper focuses on the LR-RTS algorithm and its implementation in large-scale MU-MIMO systems. Additionally, it provides a comparative analysis of LR-RTS with existing detection algorithms in terms of computational complexity and performance improvements. Ultimately, this research aims to contribute to the advancement of massive MIMO technology, making it a more viable and efficient solution for future communication challenges.

A. RELATED WORK

The core principle behind the massive MU-MIMO system is the coherent superposition of wavefronts [13]. However, realizing this system presents several signal processing challenges, impacting the trade-off between performance and complexity. The key challenges include (*i*) addressing IAI [14], (*ii*) mitigating MUI [15], (*iii*) accurately estimating CSI for a vast number of channels, (*iv*) managing synchronization, and (*v*) handling hardware implementation [16], [17]. IAI and MUI stand out as the primary bottlenecks and critical obstacles within the massive MU-MIMO system, as they significantly degrade its performance. Therefore, the primary objective of massive MU-MIMO techniques is to mitigate these interferences by using an efficient multiuser detection (MUD) that maintains computational efficiency. Many antennas within each MU's confined space are needed to meet the futuristic demands of MUs and to deliver high throughput within limited spectrum bandwidth. This arrangement, however, can lead to IAI issues. An effective pre-coding technique is employed at the transmitter to counteract IAI, facilitating detection at the receiver. The commonly used ZF and minimum mean square error (MMSE) pre-coders, while low in computational complexity, tend to yield poor bit error rate (BER) performance [18]. Non-linear pre-coders such as dirty paper coding (DPC) [19], constant envelope [20], Tomlinson–Harashima (THP) [21],

and vector-permutation (VP) [22] can achieve near-optimal BER performance. However, their computational complexities scale with the number of antennas at each MU, posing a trade-off between performance and complexity in designing pre-coding techniques for large-scale MU-MIMO systems. Hence, there is a need for a pre-coding technique that offers reduced computational demands while maintaining near-maximum likelihood (ML) performance [23].

Recently, LR-based algorithms emerged as a prominent pre-coding scheme, striking a balance between low complexity and achievable sum rate performance [24], [25], [26], [27]. The LR technique is a robust metaheuristic approach that is useful in pre-coding for massive MU-MIMO systems. It transforms the channel matrix into a nearly symmetric and more constrained channel basis within the same lattice. Consequently, it eliminates channel correlation, alleviating IAI at a MU [28]. The MUI poses another substantial challenge to the effectiveness of MU-MIMO systems [29]. This interference arises when multiple MUs are closely located, resulting in a notable similarity in the channel impulse responses (CIRs) of the MUs [30]. The CIRs act as spatial signatures for individual MUs. The MUD techniques employed at the receiver are used to tackle the impact of MUI. The primary goal of MUD schemes is to reconstruct the transmitted signal vector of the desired user from the received signal vector while effectively canceling interference stemming from undesired users. Various detection schemes have been proposed in the existing literature to combat these interferences and enhance data throughput [31], [32]. One of the notable detectors is the ZF channel inversion (ZF-CI) method [33]. Nevertheless, the ZF-CI detector yields subpar performance when the channel faces adverse conditions due to the conversion of the pre-coding vector into a non-unitary matrix, which amplifies noise. The MMSE channel inversion (MMSE-CI) method stabilizes MUI and effectively eliminates each user's noise [34]. However, it suffers from the drawback of yielding undesirable BER, particularly in large MIMO systems with higher-order modulation schemes. The matched filter channel inversion (MF-CI) detector is an alternative detector designed for channel-free environments, specifically single-input, single-output (SISO) systems [35]. Block diagonalization (BD) detectors are introduced in [36] to eliminate interferences. Nonetheless, BD detectors are complex structures primarily suited for the downlink scenario. Though the sphere decoding (SD) detector is proposed to improve BER performance, its overall complexity becomes unmanageable in the context of large MU-MIMO systems [37].

Recent research has explored search-based detectors dedicated to combating MUI issues in large-scale MU-MIMO systems, achieving complete MUI removal and effectively transforming the MU-MIMO system into a set of independent single-user MIMO (SU-MIMO) systems. Conventional MIMO linear and non-linear detectors can be employed for such SU-MIMO connections. Nguyen et al. propose time-domain multi-user interference cancellation schemes to address carrier frequency offsets (CFOs) in uplink OFDMA systems [38]. By using multiple OFDMA modulators at the base station, their method compensates for CFO impacts, significantly improving performance over conventional receivers and frequency-domain schemes, even tolerating CFOs up to 40% of subcarrier spacing. A similar approach was presented in [39] for CFO issues in uplink OFDMA. The multi-user interference cancellation scheme, using multiple OFDM demodulators, corrects and mitigates the negative effects of CFOs at the receiver, showing considerable performance gains in numerical evaluations. Bazzi and Chafii introduce a method for designing dual-functional radar and communication (DFRC) waveforms with adjustable peak-to-average power ratio (PAPR) [40]. Using the alternating direction method of multipliers (ADMM), their approach minimizes multi-user communication interference while adhering to radar chirp constraints. The method shows superior performance and adaptability to imperfect CSI in simulations. On the other hand, the LAS method operates as an iterative search-based detector that actively seeks an improved solution within the neighborhood of the signal space [42], [43], [44], [45]. Although LAS is a local and iterative approach, it outperforms ZF and MMSE detectors, although with minimal additional complexity. LAS commences with an initial solution vector, often the result of ZF or MMSE detection, and continues to refine the initial vector until saturation in improving the ML cost function is observed. In its conventional form, LAS explores the arrangement by sequentially altering each information symbol of the initial solution vector associated with all transmitting antennas. An RTS-based detection algorithm was introduced to enhance BER performance in large-scale MU-MIMO systems while minimizing computational complexity [46], [47]. RTS is an iterative search technique that delves into a local search space to explore neighborhoods and identify substantial solutions. The low-complexity RTS detector begins with an initial solution and probes the surrounding neighborhood. Even when the current solution is suboptimal, it selects the best vector among the neighboring solutions.

Most existing research has addressed either IAI or MUI, whereas this work focuses explicitly on both. Thus, this paper explores the LR-RTS MUD scheme for large-scale MU-MIMO systems, aiming to achieve near-optimal performance with less complexity.

B. CONTRIBUTIONS

This research paper makes several significant contributions to the field of large-scale MU-MIMO systems, as outlined below:

- Introduction of LR-RTS Algorithm: This paper presents the LR-RTS algorithm, which is tailored explicitly for large-scale MU-MIMO systems and effectively addresses both IAI and MUI.
- Simultaneous Mitigation of IAI and MUI: Unlike prior approaches that focus on either IAI or MUI, LR-RTS offers a unified solution, effectively tackling both

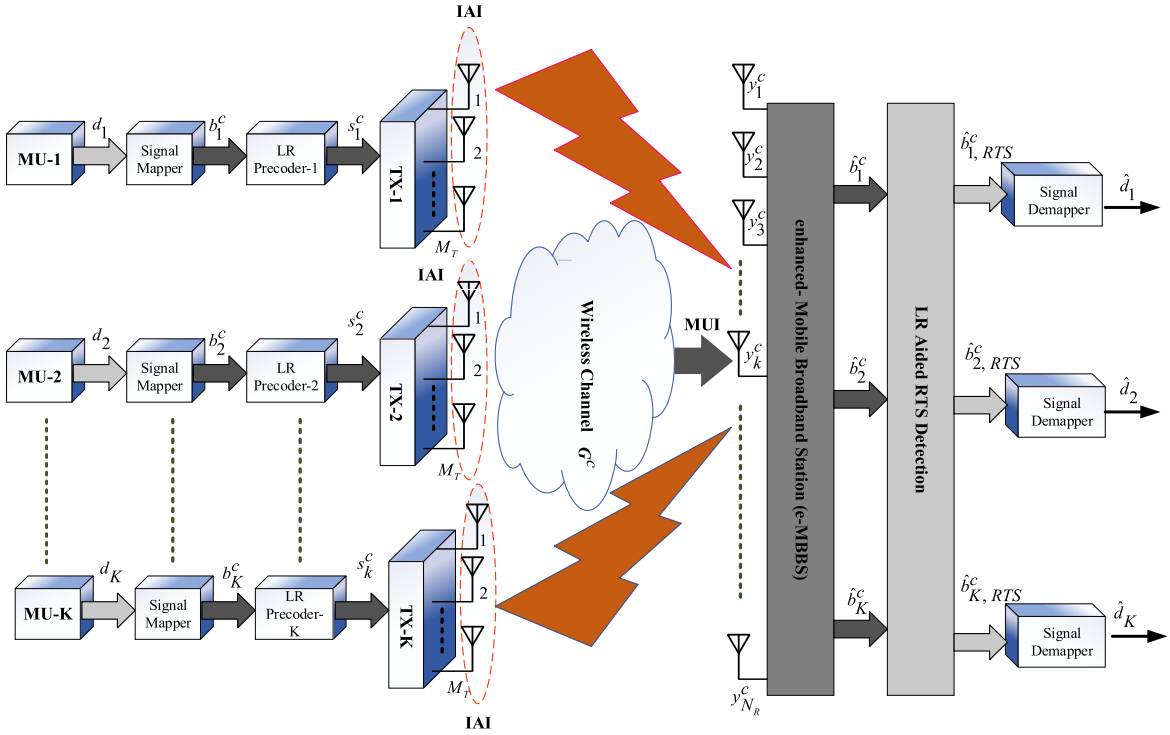

FIGURE 2. Block diagram of a proposed LR-Aided RTS detection scheme.

interferences concurrently, thereby enhancing system performance comprehensively.

- Improved Performance-Complexity Trade-off: LR-RTS achieves a refined balance between detection performance and computational complexity, delivering near-optimal results with significantly reduced computational demands compared to existing methods.
- Application to large-scale MU-MIMO systems: we showcase the effective application of our proposed method to (and its superiority in enhancing the performance of) large-scale MU-MIMO systems by means of a comprehensive comparative analysis against state-of-the-art methods, such as LAS and ZF.

This paper is structured as follows: Section II presents the mathematical model of a large-scale MU-MIMO with LR pre-coding. Section III discusses conventional MUD techniques. Section IV defines the Neighborhood Concept and introduces the search-based LR-LAS detector. Our proposed LR-based RTS detection scheme is detailed in Section V. Section VI presents simulation results and comparisons with existing techniques, while we draw our conclusions from the research findings in Section VII.

II. SYSTEM MODEL

The block diagram in Fig. 2 illustrates a proposed massive MU-MIMO system implementing hybrid LR- RTS detection. In the context of an uplink scenario within this large-scale MU-MIMO framework, the system comprises an e-MBBS equipped with a N_R substantial number of receiving antennas and K independent MUs, with each MU being equipped with its own set of transmitting antennas. Consequently, the collective count of transmitting antennas sums to the total number N_T represented by $K \times M_T$, where $N_T \leq N_R$. Here, each MU can simultaneously transmit data to the e-MBBS, which is also equipped with receiving antennas, all operating on the same channel. Given the sheer magnitude of antennas at both the e-MBBS and MUs, this system is appropriately categorized as a large-scale MU-MIMO system. The e-MBBS receiver is designed to acquire comprehensive CSI, encompassing the entire system. In contrast, each k^{th} MU is equipped to acquire its own specific CSI, which pertains to the channel between the e-MBBS and that particular MU. It is important to note that each MU remains unaware of the system's CSI associated with other MUs. Since there is no collaboration or sharing of information among different users, the CSI between the k^{th} user and the e-MBBS regarding the other $(K-1)$ users is unavailable. In the block diagram of the MU-MIMO system, the information bit vector for the k^{th} user is denoted as $\boldsymbol{d}_k = \left[\boldsymbol{d}_{k,1}, \boldsymbol{d}_{k,2}, \ldots, \boldsymbol{d}_{k,M_T}\right]^T$, where $k = 1,2,\ldots, K$.. Each $\boldsymbol{d}_{k,m}$ represents the stream of information bits used to generate the data symbol for the m^{th} antenna of the k^{th} user, and the ^{T} operation denotes the transpose operation. This vector serves as the basis for generating an un-coded complex data symbol vector $\boldsymbol{b}_k^c = \left[b_{k,1}, b_{k,2}, \ldots, b_{k,M_T}\right]^T \in C^{M_T}$. These un-coded symbol vectors are subsequently processed and encoded as $\boldsymbol{s}_k^c$ through LR pre-coding, effectively mitigating IAI encountered at each MU. The resulting complex pre-coded signal vector

$\boldsymbol{s}_k^c = \left[s_{k,1}, s_{k,2}, \ldots, s_{k,M_T}\right]^T \in C^{M_T}$ is then transmitted over M_T transmitting antennas through a user-specific complex channel G_k^c, representing the channel coefficient matrix between the e-MBBS and the k^{th} MU.

The complex channel coefficient matrix is denoted as:

$$\boldsymbol{G}_k^c = \begin{bmatrix} g_{11}^k & g_{12}^k & \cdots & g_{1M_T}^k \\ g_{21}^k & g_{21}^k & \cdots & g_{2M_T}^k \\ \vdots & \vdots & \ddots & \vdots \\ g_{N_R1}^k & g_{N_R2}^k & \cdots & g_{N_RM_T}^k \end{bmatrix} \tag{1}$$

With this channel matrix, the $(N_R \times 1)$-dimensional complex received signal vector at the e-MBBS from K concurrent MUs is mathematically expressed as follows:

$$\boldsymbol{y}^c = \sum_{k=1}^{K} \boldsymbol{G}_k^c \boldsymbol{s}_k^c + \boldsymbol{w}^c, \tag{2}$$

where $\boldsymbol{w}^c = \left[w_1, w_2, \ldots, w_{N_R}\right]^T$ is an $(N_R \times 1)$-dimensional vector consisting of independent and identically distributed Additive White Gaussian noise (AWGN) with a zero mean and variance σ_w^2. For convenience, the complex MIMO system model presented in (2) is transformed into an equivalent real-valued system as follows:

$$\boldsymbol{y} = \sum_{k=1}^{K} \boldsymbol{G}_k \boldsymbol{s}_k + \boldsymbol{w}, \tag{3}$$

where

$$\boldsymbol{s}_k = \left[\text{Re}(\boldsymbol{s}_k^c)^T \ \text{Im}(\boldsymbol{s}_k^c)^T\right]^T \in \mathbb{R}^{2M_T \times 1},$$
$$\boldsymbol{y}_k = \left[\text{Re}(\boldsymbol{y}_k^c)^T \ \text{Im}(\boldsymbol{y}_k^c)^T\right]^T \in \mathbb{R}^{2N_R \times 1},$$
$$\boldsymbol{c} = \left[\text{Re}(\boldsymbol{c}^c)^T \ \text{Im}(\boldsymbol{c}^c)^T\right]^T \in \mathbb{R}^{2N_R \times 1}$$
$$\text{and } \boldsymbol{G}_k = \begin{bmatrix} \text{Re}(\boldsymbol{G}_k^c) & -\text{Im}(\boldsymbol{G}_k^c) \\ \text{Im}(\boldsymbol{G}_k^c) & \text{Re}(\boldsymbol{G}_k^c) \end{bmatrix} \in \mathbb{R}^{2N_R \times 2M_T}.$$

In this context, Re(.) and Im(.) indicate the real and imaginary components, respectively.

A. LR PRE-CODING ALGORITHM

IAI can significantly degrade the Signal-to-Interference-plus-Noise Ratio (SINR) in MIMO systems, leading to reduced data rates, decreased reliability, and impaired spectral efficiency. By mitigating IAI through precoding techniques, we aim to alleviate these adverse effects and enhance the overall performance of MIMO systems. LR serves as an effective pre-coding strategy designed to enhance the performance of large-scale MU-MIMO systems while significantly reducing computational demands. This technique relies on CSI at each UE, denoted as $\boldsymbol{G}_k$. The primary objective of LR is to transform the given channel basis vector, $\boldsymbol{G}_k$, into a novel basis vector situated within the shortest Euclidean space. When $\boldsymbol{G}_k$ comprises an orthogonal lattice basis vector, the decision boundary region of the linear system closely aligns with that of the ML system. As a result, the orthogonality within a lattice basis vector has a profound impact on the performance of the large-scale MU-MIMO receiver. Various channel vectors can commence with the same lattice basis, facilitating the design of nearly orthogonal bases $\hat{\boldsymbol{G}}_k$ for a corresponding lattice basis vector $\boldsymbol{G}_k$. Within the framework of LR pre-coding, channel coefficients take on the role of lattice points, and these lattices are refined into improved lattices through the well-established Lenstra, Lenstra, and Lovász (LLL) reduction algorithm. This algorithm, known for its efficiency as a suboptimal reduction technique, swiftly identifies the nearest shortest basis vector within any lattice in polynomial time complexity. By harnessing the power of the LLL algorithm, the original channel matrix $\boldsymbol{G}_k$ is transformed into a new equivalent channel matrix, denoted as $\hat{\boldsymbol{G}}_k$, as follows:

$$\hat{\boldsymbol{G}}_k = \boldsymbol{G}_k \boldsymbol{T}, \tag{4}$$

where $\boldsymbol{T}$ stands for an unimodular transformation matrix attained through the LLL algorithm, and each element within $\boldsymbol{T}$ belongs to the set of Gaussian integers.

A lattice constitutes an assortment of distinct vectors, specifically the columns forming the channel matrix of the k^{th} MU, denoted as $L(\boldsymbol{G}_k)$. In a real-valued channel matrix, $\boldsymbol{G}_k$ can be represented through a collection of linearly independent basis vectors, commonly referred to as lattice basis. Consequently, the lattice can be defined as:

$$L\left(\boldsymbol{G}_k\right) = L\left(\boldsymbol{g}_1, \boldsymbol{g}_2, \ldots, \boldsymbol{g}_{2M_T}\right) = \boldsymbol{G}_k \boldsymbol{s}_k, \tag{5}$$

where $\boldsymbol{g}_i,\ i = 1, 2, \ldots, 2M_T$ represents the i^{th} column of the k^{th} MU's channel matrix. This lattice undergoes a transformation process, resulting in a new lattice denoted as $L(\hat{\boldsymbol{G}}_k)$, wherein the transformed channel $\hat{\boldsymbol{G}}_k$ is obtained through a series of elementary column operations. These operations encompass sign reflection, column swapping, and column translation, all applied to the original channel matrix $\boldsymbol{G}_k$ [18]. Collectively, these elementary column operations yield an unimodular matrix $\boldsymbol{T}_k$ with dimensions $(2M_T \times 2M_T)$. This unimodular matrix allows us to express $\hat{\boldsymbol{G}}_k$ as a product of $\boldsymbol{G}_k$ and $\boldsymbol{T}_k$. Importantly, the unimodular matrix exclusively comprises integer elements, with a determinant $\det(\boldsymbol{T}_k)$ equal to either $+1$ or -1. The transformed channel, a result of these elementary column operations, maintains the same lattice structure $L(\hat{\boldsymbol{G}}_k) = L(\boldsymbol{G}_k)$. It is worth noting that the inverse of unimodular matrices also exists and consists entirely of integer values $\boldsymbol{T}_k^{-1} \in \mathbb{Z}^{2M_T \times 2M_T}$, enabling us to define $\boldsymbol{G}_k$ as $\hat{\boldsymbol{G}}_k \boldsymbol{T}_k^{-1}$. The expression for the received signal, as provided in (3), is now adapted for a Large-Scale MU-MIMO system with LR pre-coding, and it is articulated as follows

$$\boldsymbol{y}_{LR} = \sum_{k=1}^{K} \boldsymbol{G}_k \boldsymbol{T}_k \boldsymbol{T}_k^{-1} \boldsymbol{s}_k + \boldsymbol{w} = \sum_{k=1}^{K} \hat{\boldsymbol{G}}_k \boldsymbol{b}_k + \boldsymbol{w}, \tag{6}$$

where $\boldsymbol{b}_k = \boldsymbol{T}_k^{-1} \boldsymbol{s}_k$ and $\boldsymbol{s}_k$ represent the $(2M_T \times 1)$-dimensional real-valued un-coded and pre-coded signal vectors of the k^{th} MU, respectively.

III. CONVENTIONAL MUD SCHEMES

Numerous detection schemes have been put forth in the existing body of literature, as elaborated below. Among these, the ML can recover the transmitted symbol vector $\boldsymbol{s}$ from all $\mathbb{A}^{2N_T}$ potential transmitted vectors that closely approximate the received signal vector $\boldsymbol{y}$, considering the specific channel matrix $\boldsymbol{G}$, which can be expressed as:

$$\hat{\boldsymbol{s}}_{ML-D} = \underset{\boldsymbol{s}\in\mathbb{A}^{2N_T}}{\arg\min} \|\boldsymbol{y} - \boldsymbol{G}\boldsymbol{s}\|^2, \tag{7}$$

where, $\boldsymbol{G} = [\boldsymbol{G}_1, \boldsymbol{G}_2, \ldots, \boldsymbol{G}_K]$ is the overall channel matrix, ||. || represents L_2 norm. The ML cost function is defined as:

$$\phi(\boldsymbol{s}) = \|\boldsymbol{y} - \boldsymbol{G}\boldsymbol{s}\|^2 = \sum_{i=1}^{2N_R} \left| y_i - \sum_{j=1}^{2N_T} g_{ij} s_j \right|^2, \tag{8}$$

While the ML detector is a powerful technique, it becomes impractical for large MU-MIMO systems due to its exponential computational complexity. In such cases, alternative detectors with lower accuracy, such as the matched filter (MF), ZF, and MMSE detectors, are employed to mitigate MUI while maintaining a more manageable computational complexity. The mathematical expressions for detecting the real-valued symbol vector $\hat{\boldsymbol{s}} = \left[\hat{\boldsymbol{s}}_1^T, \hat{\boldsymbol{s}}_2^T, \ldots, \hat{\boldsymbol{s}}_K^T\right]^T$, where $\hat{\boldsymbol{s}}_k = \left[\mathrm{Re}\left(\hat{\boldsymbol{s}}_k^c\right)^T \mathrm{Im}\left(\hat{\boldsymbol{s}}_k^c\right)^T\right]^T$, using these various detectors, are provided as follows

$$\hat{\boldsymbol{s}}_{MF-D} = \boldsymbol{G}^H \boldsymbol{y}, \tag{9}$$

$$\hat{\boldsymbol{s}}_{ZF-D} = \left(\boldsymbol{G}^H \boldsymbol{G}\right)^{-1} \boldsymbol{G}^H \boldsymbol{y}, \tag{10}$$

$$\hat{\boldsymbol{s}}_{MMSE-D} = \left(\boldsymbol{G}^H \boldsymbol{G} + \sigma_n^2 I\right)^{-1} \boldsymbol{G}^H \boldsymbol{y}. \tag{11}$$

Conventional MUD detectors achieve a uniform signal-to-noise ratio (SNR) for all detectors. However, reducing the MUI separately is difficult, leading to performance-complexity trade-offs between the systems, especially for large MU-MIMO systems.

IV. SEARCH-BASED DETECTION TECHNIQUES

Neighbor search-based detection schemes have been proposed to achieve better BER performance with less computational complexity, as discussed below.

A. NEIGHBORHOOD DEFINITION

The pre-coded symbol vector $\boldsymbol{s}$ contains L neighborhood symbols $O_L(\boldsymbol{s})$, which are as follows: Let us define a symbol vector $\hat{\boldsymbol{s}}$, where $\hat{\boldsymbol{s}} \in O_L(\boldsymbol{s})$. Then, there will be a total of $\binom{2N_T}{L}$ possible symbols for such $\hat{\boldsymbol{s}}$. The sets of indices at which $\boldsymbol{s}$ and $\hat{\boldsymbol{s}}$ vary are represented by I_k, where $k = 1, 2, \ldots, \binom{2N_T}{L}$. A neighborhood vector $\hat{\boldsymbol{s}} \in O_L(\boldsymbol{s})$ is:

$$\hat{s}_i = \begin{cases} \varphi_j, & \varphi_j \in \phi \ \ and \ \ i \in I_k, \forall \varphi_j \neq s_i \\ s_i, & i \notin I_k, \end{cases} \tag{12}$$

where $\varphi = \left\{\pm 1, \pm 3, \ldots, \pm\left(\sqrt{b} - 1\right)\right\}_{2N_T \times 1}$, i takes values from 1 to $2N_T$, and j ranges from 1 to L. Thus, the total number of vectors in $O_L(\boldsymbol{s})$ amounts to $\left(\sqrt{b} - 1\right)^L \binom{2N_T}{L}$. To illustrate this concept, let's consider a 16-QAM modulation scheme, where the real equivalent constellation set φ is characterized by {–3, –1, 1, 3}, and a symbol vector $O_L(-3)$ is formed with a length of 3, comprising {–1, 1, 3}. The 1-symbol neighborhood of this $O_L(\boldsymbol{s})$ vector can be created by sequentially modifying each element, one at a time, with the other elements from the φ set. For instance, with regard to the first element of the symbol vector, we generate 3 vectors in the 1-symbol neighborhood: [–1, 3, –1], [3, –1,3], and [3, 3, –1]. A similar process is applied to the other two locations, generating an additional 6 symbol vectors. Consequently, two optimal neighborhood sets for each symbol within φ can be defined as follows: $O_L(-3) = \{-1, 1\}$, $O_L(-1) = \{-3, 1\}$, $O_L(1) = \{-1, 3\}$, and $O_L(1) = \{1, -1\}$. This theory can be extended to all symbol vectors, resulting in M neighborhood vectors for each symbol vector, where $M = |O_L(\boldsymbol{s})|$. The minimum and maximum values for M are set to 1 and $L - 1$, respectively.

Considering the definition of neighborhood, various versions of LAS algorithms emerge, such as 1-LAS, multiple LAS (MLAS), multiple output selection LAS, and RTS. These neighborhood-based algorithms primarily aim to identify the best vector, which represents the symbol vector with the minimum Euclidean distance, among the neighborhood candidates. However, a significant challenge lies in selecting the initial solution vector and defining the search space. Typically, linear detectors are chosen as initial solution vectors. An LR-ZF detector is considered to improve the initial solution vector's quality, as the hard decisions made by the LR-ZF detector tend to be more reliable than the linear detectors. Further details regarding this will be discussed in the subsequent section

B. LATTICE REDUCTION ASSISTED LIKELIHOOD ASCENT SEARCH (LR-LAS) DETECTOR

In the context of large-scale MU-MIMO systems, the MUI stemming from these simultaneous MUs tends to be more conspicuous than the IAI. Consequently, the performance of conventional detectors becomes notably constrained. While the ML detector delivers superior BER performance, its computational complexity exceeds the capabilities of large-scale MU-MIMO systems. Therefore, the challenge lies in devising nearly optimal detectors with minimal complexity, a pivotal consideration for the practical deployment of large-scale MU-MIMO systems. In this context, the low-complexity LAS detector emerges as an attractive solution, as its performance closely rivals that of the ideal ML detector. The LAS detector initializes its search process with the aid of the ZF detector vector, subsequently exploring the neighborhood solution space around the initial solution vector. This initial solution for the LAS detector consists of neighborhood symbols that yield the lowest ML cost value.

Let

$$\hat{\boldsymbol{s}}_{LR-ZF} = \left[(\hat{\boldsymbol{s}}^1)^T, (\hat{\boldsymbol{s}}^2)^T, \ldots, (\hat{\boldsymbol{s}}^K)^T\right]^T = \left[\hat{s}_1, \hat{s}_2, \ldots, \hat{s}_{2N_T}\right]^T,$$

be the real-valued solution attained from LR-assisted ZF detector and is defined as:

$$\hat{\boldsymbol{s}}_{LR-ZF} = \left(\hat{\boldsymbol{G}}^H \hat{\boldsymbol{G}}\right)^{-1} \hat{\boldsymbol{G}}^H \boldsymbol{y}_{LR}. \tag{13}$$

where, $\hat{\boldsymbol{G}} = [\hat{\boldsymbol{G}}_1, \hat{\boldsymbol{G}}_2, \ldots, \hat{\boldsymbol{G}}_K]$ is the overall transformed channel matrix. Let $\boldsymbol{O} = [\boldsymbol{o}_1, \boldsymbol{o}_2, \ldots, \boldsymbol{o}_L]$ be the set consisting of all possible trail vectors, where $\boldsymbol{o}_j = \left[o_{1,j}, o_{2,j}, \ldots, o_{2M_T,j}\right]^T, j = 1, 2, \ldots, L$. If the n^{th} symbol is the intended symbol, the elements of the trial vector $\boldsymbol{O}_{\text{L}}$ are selected in accordance with the following

$$o_{i,j} = \begin{cases} \varphi_j \ \ if \ \ i = n \\ \hat{s}_i \ \ if \ \ i \neq n, \end{cases} \quad \text{where } j = 1, 2, \ldots, L \text{ and } i = 1, 2, \ldots, 2N_T \tag{14}$$

Thus, the estimation of the n^{th} data symbol is obtained through the LR-LAS detector as follows

$$\hat{\boldsymbol{s}}_{n,\, LR-LAS} = \arg \min_{\boldsymbol{s}=\boldsymbol{o}_j, j=1,2,\ldots,L} \|\boldsymbol{y} - \boldsymbol{G}\boldsymbol{s}\|^2, n = 1, 2, \ldots, 2N_T. \tag{15}$$

The LR-LAS detector requires the evaluation of $(L \times 2N_T)$ ML cost functions to detect all users. The performance of the LAS detector is primarily influenced by two key parameters: the selection of the initial solution vector and the definition of the search space. LAS can attain superior BER performance with reduced computational complexity when an appropriate initial solution is chosen. Nonetheless, a major challenge for LAS is the early termination problem, primarily due to its relatively limited search space, which is impractical for extensive constellations and massive MU-MIMO systems. To address this challenge and achieve the best error rate performance with minimized computational load, we introduce the LR-RTS detector in this study.

V. PROPOSED LATTICE REDUCTION ASSISTED REACTIVE TABU SEARCH (LR-RTS) DETECTOR

Reactive Tabu Search represents an iterative and heuristic detection approach that heavily relies on local neighborhood exploration. It offers notably superior performance, particularly in the context of large-scale MU-MIMO systems, often involving a substantial number of antennas, ranging from tens to several thousand. Much like the LAS method, the RTS algorithm commences its operations with an initial solution vector. Typically, this initial vector is provided by the LR-ZF detector. The algorithm then establishes a neighborhood symbol vector based on specific criteria, subsequently transitioning to the best neighboring vector within that neighborhood. If, during this transition, the best neighboring vector results in a higher ML cost function value, the current solution vector is preserved as the initial solution. This strategy helps the algorithm escape local minima. The entire process persists for a predetermined number of iterations, with the best solution vector across all these iterations ultimately recognized as the final solution vector. This approach introduces a unique aspect wherein solution vectors from the preceding few iterations, often referred to as "Tabu," play a crucial role in defining the neighborhood for the solution vector in a particular iteration. By doing so, the RTS algorithm effectively navigates the solution space while adhering to a "Tabu period," which represents the cumulative number of these preceding iterations. The overall sequence of the RTS algorithm unfolds as follows.

A. REACTIVE TABU SEARCH (RTS) ALGORITHM

The RTS algorithm commences with an initial solution vector $\hat{\boldsymbol{s}}^{(0)}_{ZF-D}$ derived from the ZF detector as given in (13). To generate the best initial solution vector, we propose the LR-associated ZF (LR-ZF) detector $\hat{\boldsymbol{s}}^{(0)}_{LR-ZF}$ as an initial solution. Create all neighborhood symbol vectors using the $\hat{\boldsymbol{s}}^{(0)}_{LR-ZF}$, and define the maximum number of iterations $\tau_{\max}$. Later, the ML cost functions of each neighborhood vector are determined, and the best neighborhood vector among all (lowest ML cost metrics) is selected. The RTS algorithm supports both local and global solutions. At first, the initial solution is treated as a global solution. The best neighborhood vector updates the global solution. During each iteration of the RTS algorithm, indexed as k (where $k = 1, 2, \ldots, \tau_{\max}$), if the value of the ML cost function is found to be lower than the cost of the global solution, the best neighborhood vector is utilized to enhance the global solution. The ML cost function for the global solution is then updated to match the best neighborhood cost function. Conversely, suppose the best neighborhood cost function at the kth iteration surpasses the cost function of the global solution. In that case, the move of the equivalent neighborhood vector is stored in the tabu matrix at specified intervals. This strategic limitation of moves at defined intervals is crucial in helping the RTS algorithm steer clear of local minima. In both scenarios, the initial solution for the subsequent iteration is configured as the best neighborhood vector, followed by the update of the tabu matrix and the tabu period. Ultimately, the RTS algorithm is concluded when the established condition is met. Otherwise, once again, it creates all neighborhood symbol vectors with the help of the initial solution vector $\hat{\boldsymbol{s}}^{(0)}_{LR-ZF}$. The data symbol vector belonging to the real-valued solution attained from LR assisted ZF detector at k^{th} iteration is defined as

$$\begin{aligned} \hat{\boldsymbol{s}}^k_{LR-ZF} &= [(\hat{\boldsymbol{s}}^k_1)^T, (\hat{\boldsymbol{s}}^k_2)^T, \ldots, (\hat{\boldsymbol{s}}^k_{2N_T})^T]^T \\ &= [\hat{\boldsymbol{s}}^k_1, \hat{\boldsymbol{s}}^k_2, \ldots, \hat{\boldsymbol{s}}^k_{2N_T}]^T, \end{aligned} \tag{16}$$

where $\hat{s}^k_i = O_L(s), L \in \{1, 2, \ldots, 2_{N_T}\}$ and the neighborhood vector of $\hat{\boldsymbol{s}}^k_{LR-ZF}$ is defined as

$$\boldsymbol{Q}^k(u, v) = \left[q^k_1(u, v)^T, q^k_2(u, v)^T, \ \ldots, q^k_{2N_T}(u, v)^T\right]^T, \tag{17}$$

where $u = 1, 2,\ldots,2N_T$ and $v = 1, 2,\ldots, M$. The neighboring vector is defined as

$$q_i^k(u, v) = \begin{cases} \hat{s}_i^k, & \text{for } i \neq u \\ \varphi_v\left(\hat{s}_u^k\right), & \text{for } i = u. \end{cases} \tag{18}$$

As a result, there will be $2MN_T$ vectors in the solution space and only one coordinate different from the given vector. The neighborhood of the provided vector is prepared from these $2MN_T$ vectors. A move is an operation on $\hat{\boldsymbol{s}}_{LR-ZF}^k$ that produces $\hat{\boldsymbol{s}}_{LR-ZF}^{k+1}$ which is a member of $\hat{\boldsymbol{s}}_{LR-ZF}^k$ vector neighborhood. If $\hat{\boldsymbol{s}}_{LR-ZF}^{k+1} = \boldsymbol{Q}^k(u, v)$, the algorithm is said to have executed the move (u, v). Therefore, some $2MN_T$ candidates can be considered for a move during any given iteration. Additionally, the cardinality of the union of all moves from all L^{2N_T} potential solution vectors is $2LMN_T$, which is the total number of conceivable '' distinct '' moves. A move cannot be considered for that many additional iterations if its ''Tabu'' value is a non-negative integer.

B. TABU MATRIX CALCULATION AND STOPPING CRITERION

The matrix whose elements represent the Tabu values of moves is called a Tabu matrix τ and has the dimension $2LMN_T$. The solution vector contains $2N_T$ coordinates, and each coordinate of the solution vector consists of L rows in a Tabu matrix τ where $\boldsymbol{\tau} \in O_L(\boldsymbol{s})$. The indices of the rows corresponding to the u coordinate are from $(u-1)L+1$ to uL, where $u \in \{1, 2,\ldots, 2N_T\}$. The M columns of the Tabu matrix τ represent the symbol neighborhoods of the symbols corresponding to each row. In other words, the $(p, r)^{\text{th}}$ entry of the matrix τ corresponds to the $(u, v)^{\text{th}}$ entry of $\hat{\boldsymbol{s}}_{LR-ZF}^k$, where $u = \left[\frac{p-1}{L}\right]+1$ and $v = r$, where $p = 1, 2,\ldots, 2LN_T$ and $r = 1, 2,\ldots, M$. The entries of the Tabu matrix are upgraded in each iteration are described as:

$$\boldsymbol{\tau}(p, r) = \max\{\boldsymbol{\tau}(p, r) - 1, 0\}. \tag{19}$$

The Tabu matrix is terminated if it reaches the maximum number of iterations $\tau_{\max}$. Additionally, the method is terminated if the current solution is a local minimum and the overall number of solution repetitions exceeds $\tau_{\max}$. The n^{th} data symbol is assessed from the LR-RTS detector as

$$\hat{\boldsymbol{s}}_{n,LR-RTS} = \arg \min_{\substack{\boldsymbol{s}=q(u,v),\ u=1,2,\ldots,2N_T \\ v=1,2,\ldots,M}} \left\|\boldsymbol{y}_{LR} - \hat{\boldsymbol{G}}\boldsymbol{s}\right\|^2, \quad n = 1, 2, \ldots, 2N_T \tag{20}$$

The LR-RTS detector evaluates the $(2LMN_T)$ number of ML cost functions to detect all users. The vector with the lowest ML cost function when the algorithm was stopped would, therefore, be the vector representing the algorithm's solution. The RTS algorithm can attain near-optimal performance for large MIMO systems and higher-order modulation schemes. Moreover, it has been demonstrated that the average per-bit complexity RTS is $O(N_T N_R)$, thus making it appealing for large-MIMO signal detection.

Algorithm 1 Lattice Reduction Associated Reactive Tabu Search Detection (LR-RTS-Detection)

Step 1: Initialize the system parameters
Inputs: $\boldsymbol{s}, \boldsymbol{G}, \boldsymbol{b}, i, j, L, M, O, k, \varphi, r, u. v. p, \tau, \boldsymbol{y}$
Output: $\hat{\boldsymbol{s}}_{n,LR-RTS}$
Step 2: Generate LLL based LR precoding Scheme
for $k = 1$ to K;
$\boldsymbol{G}_k\boldsymbol{T}_k \leftarrow \hat{\boldsymbol{G}}_k$; LLL-based LR precoding
$\boldsymbol{T}_k^{-1}\boldsymbol{s}_k \leftarrow \boldsymbol{b}_k$; LR precoding Signal Vector
$\left(\boldsymbol{G}^H\boldsymbol{G}\right)^{-1}\boldsymbol{G}^H\boldsymbol{y} \leftarrow \hat{\boldsymbol{s}}_{ZF-D}$; LR solution vector
end for
Step 3: Generate the neighbourhood signal vector based on the LR-ZF solution vector treated as an initial solution vector.
$[o_1(\boldsymbol{s}), o_2(\boldsymbol{s}), \ldots\ldots, o_L(\boldsymbol{s})] \leftarrow O_L(\boldsymbol{s})$
$[\varphi_1, \varphi_2, \ldots\ldots, \varphi_{2N_T}] \leftarrow \varphi$
if $i = n$
$\varphi_j \leftarrow O_{i,j}$
else
$O_{i,j} \leftarrow \hat{\boldsymbol{s}}_i$
end
Step 4: Calculate and Upgrade the Tabu matrix.
for $p = 1, 2,\ldots, 2N_T L$
for $r = 1, 2,\ldots, M$
if
$\boldsymbol{\tau} \leftarrow O_L(\boldsymbol{s})$
else
$\boldsymbol{\tau}(p, r) = max\{\boldsymbol{\tau}(p, r) - 1, 0\}$
end if
end for
end for
Step 5: Define the initial solution vector
$[\hat{\boldsymbol{s}}_1^k, \hat{\boldsymbol{s}}_2^k, \ldots, \hat{\boldsymbol{s}}_{2N_T}^k]^T \leftarrow \hat{\boldsymbol{s}}_{LR-ZF}^k$
Step 6: Choose the best neighbourhood vector from the initial solution which has the lowest cost among all neighbours.
for $u = 1$ to $2N_T$
for $v = 1$ to M
if $i = u$
$q_i^k(u, v) \leftarrow \varphi_v\left(\hat{s}_u^k\right)$
else
$q_i^k(u, v) \leftarrow \hat{\boldsymbol{s}}_i^k$
end if
end for
end for
Step 7: Generate the final LR RTS solution Vector
for $n = 1, N_T$
$\arg \min_{\substack{\boldsymbol{s}=q(u,v),\ u=1,2,\ldots,2N_T \\ v=1,2,\ldots,M}} \|\boldsymbol{y} - \boldsymbol{G}\boldsymbol{s}\|^2 \leftarrow \hat{\boldsymbol{s}}_{n,LR-RTS}$
end for

VI. SIMULATION RESULTS

The simulation analysis focuses on an uplink model of a large-scale MU-MIMO system, where the MUs serve as transmitters, and the e-MBBS as receivers. In the simulation results, the proposed LR-RTS detector's performance is systematically compared with the average BER of each MU, obtained using various traditional detectors such as ZF, LR-ZF, ZF-LAS, LR-LAS, and SISO-AWGN detectors. These performance metrics are averaged over 100 data frames, each consisting of 1000 data symbols, to ensure the reliability and accuracy of the results.

TABLE 1. Simulation parameters.

Parameter	Value
Receiving antennas at e-MBBS (N_R)	128
MUs count (K)	16
Antennas per MU (M_T)	8
Data frames count	100
Symbols per each data frames	1000
Range of SNR	-10 dB to 15 dB
Modulation type	4-QAM, 16–QAM, and 64 QAM
Wireless channel type	Rayleigh flat fading
LR reduction parameter (δ)	3/4
Maximum number of iterations in LLL algorithm	4
Initial vector of RTS	LR-ZF
Initial value of the Tabu period	2
Adaptation constant of RTS	0.1
Maximum number of repetitions allowed in RTS (k)	50

The simulation assumes that multiple MUs transmit their data over a block fading channel, which remains constant during the transmission of a single full data frame. The channel matrix comprises complex random elements that are statistically independent, resembling a Rayleigh flat fading channel [45]. Table 1 includes the other critical parameters used in the evaluation process to provide a comprehensive view of the simulation setup.

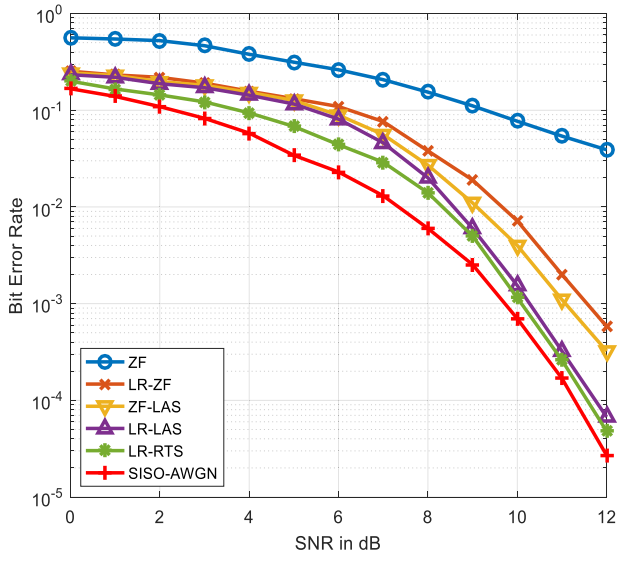

FIGURE 3. BER performance comparison among LR-RTS and conventional MUDs.

A. PERFORMACE STUDY

This section evaluates the error rate performance of LR-RTS detection and compares it with traditional detectors in large-scale MU-MIMO systems, with each user employing a 4-QAM modulation scheme, as illustrated in Fig. 3. In such systems, ZF detection exhibits sub-optimal performance, especially in high SNR scenarios while mitigating MUI, resulting in higher BER. On the other hand, LR-RTS leverages lattice reduction, outperforming ZF by enhancing BER. LR-ZF combines ZF with lattice reduction for better performance. ZF-LAS adds search-based optimization to ZF, with LR-RTS often surpassing it by employing lattice reduction and advanced search strategies. LR-LAS combines lattice reduction with LAS optimization, with LR-RTS potentially offering better BER due to its specific search strategy and refined lattice reduction. LR-RTS also excels in a simplified SISO-AWGN scenario, further improving BER compared to LR-ZF. LR-RTS significantly enhances BER compared to the baseline in MU-MIMO systems, where MUI is a challenge. The improved BER in LR-RTS is attributed to lattice reduction and the reactive Tabu search-based optimization. Lattice reduction transforms the channel matrix favorably, and the reactive Tabu search efficiently explores the solution space, yielding superior solutions in large-scale MU-MIMO systems. Fig. 3 reveals that the classical ZF detector mitigates partial MUI but doesn't nullify IAI, while LR-ZF suppresses partial MUI after nullifying IAI, resulting in better performance. In such systems, MUI's importance exceeds that of IAI, and the LR–LAS detector excels in reducing high MUI, outperforming ZF and LR-ZF. LR-RTS consistently outperforms all classical detectors, achieving a 2 dB SNR for a 10^{-1} BER level, while ZF, LR-ZF, ZF-LAS, LR-LAS, and SISO detectors require 9 dB, 7 dB, 6 dB, 5 dB, and 2 dB, respectively.

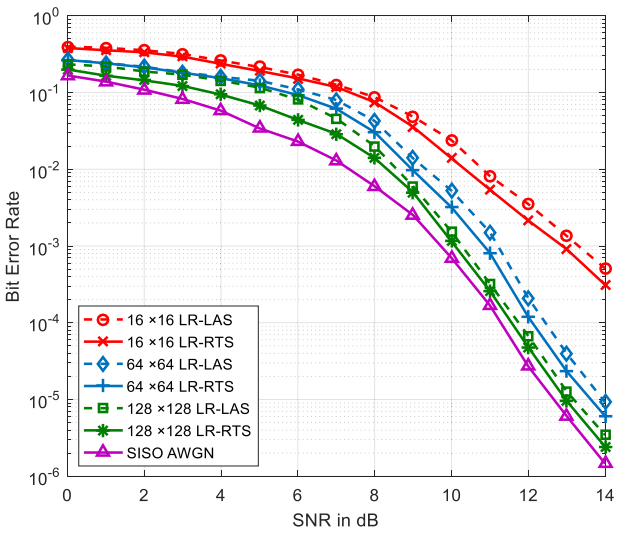

FIGURE 4. BER performance of LR-RTS for different antenna configurations.

In Fig. 4, we examine the BER performance of neighborhood search-based detection schemes, specifically LR-LAS and the proposed LR-RTS, with each user employing 4-QAM modulation. We analyze these performance outcomes across different antenna configurations, namely 16×16, 64×64, and 128×128, as displayed in Fig. 4. With an increase in antennas, the MUI in the system also rises, resulting in a gradual

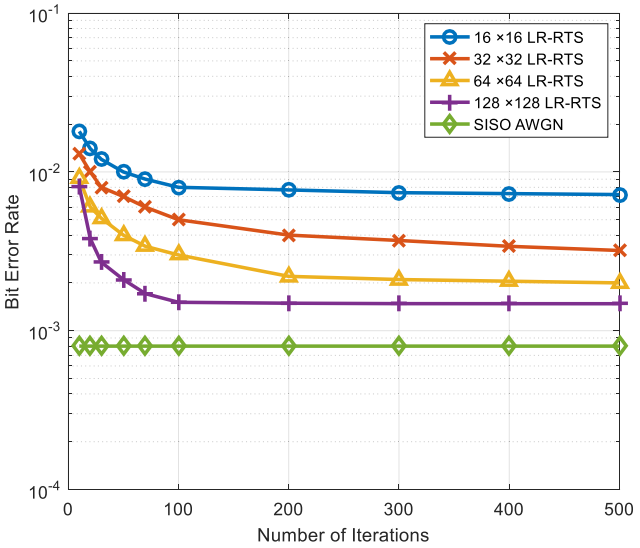

FIGURE 5. Convergence of LR-RTS for different antenna configurations.

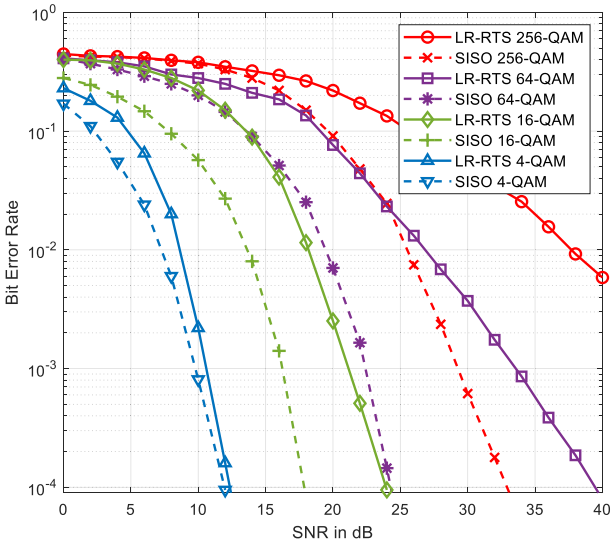

FIGURE 6. BER performance of LR-RTS for different modulation techniques.

increase in BER. However, when compared to the LR-LAS detector, the proposed LR-RTS boasts a significantly larger search space, enabling it to effectively mitigate both IAI and MUI, thereby achieving near-optimal performance. This analysis is vividly illustrated in Fig. 4. For instance, when accommodating 16×16, 64×64, and 128×128 antenna configurations at an 8dB SNR, the LR-LAS detector yields BER values of 0.087, 0.0426, and 0.02, respectively. In contrast, the proposed LR-RTS detector achieves BER values of 0.075, 0.031, and 0.014, respectively, which closely approximates the BER performance of a SISO system, which records a BER of 0.006, as shown in Fig. 4.

Figure 5 offers a detailed view of how the proposed LR-RTS detector converges across different antenna configurations. This analysis focuses on the impact of the maximum number of tabu iterations ($\tau_{\max}$) on the detector's performance. It becomes clear that the effectiveness of the RTS detector is closely tied to the choice of the search space. When the search space is larger, the RTS detector achieves improved (BER performance while requiring fewer computational resources. Fig. 5 illustrates the BER performance for various scenarios, including SISO and antenna configurations of 16×16, 32×32, 64×64, and 128×128. With 300 iterations ($\tau_{\max}=300$), the proposed LR-RTS detector delivers BER results of 0.00253, 0.005, 0.009648, 0.02468, and 0.0358 for the respective configurations. This information underscores the impact of the search space size on the efficiency of the LR-RTS detector and its ability to deliver low BER values across different antenna setups.

Furthermore, it is crucial to examine the SNR differences between the proposed LR-RTS detector and the SISO system across various QAM schemes, as illustrated in Fig. 6. This analysis helps us understand the impact of modulation choices on the required SNR to sustain a BER threshold of 10^{-3}. Fig. 6 reveals intriguing insights, showing significant SNR variations for different QAM modulation schemes when targeting a 10^{-3} BER floor. Specifically, the SNR improvements of the LR-RTS detector over SISO-AWGN are approximately 1 dB, 5 dB, 9 dB, and 17 dB for 4-QAM, 16-QAM, 64-QAM, and 256-QAM, respectively. These findings, depicted in Fig. 6, highlight the varying SNR requirements based on the modulation scheme, providing valuable information for optimizing communication systems.

TABLE 2. Comparative analysis of detectors regarding the assessment of ML cost function calculations.

MUD	Complexity Order	Complexity		
		4-QAM	16-QAM	64-QAM
LR–LAS	$L\times 2N_T$	1.024×10^3	4.096×10^3	1.638×10^4
LR–RTS	$K\times L^{2M_t}$	6.871×10^{10}	2.951×10^{20}	1.267×10^{30}
ML	L^{2N_t}	1.340×10^{154}	1.797×10^{308}	2.41×10^{462}

B. COMPUTATIONAL STUDY

We conducted a comparative study involving the LR-RTS detector, ZF-LAS, and ML detectors, focusing on their respective computational intricacies, as delineated in Table 2. This table provides a metric for evaluating computational complexity, quantifying the number of cost function calculations needed for the ML detectors. Further, Table 3 illustrates the implementation complexity in terms of the count of additions and multiplications. It is worth noting that the ZF-LAS scheme demonstrated notably low computational complexity. ZF-LAS accomplishes its solution through localized searches at each transmitting antenna, rendering it relatively computationally efficient. In sharp contrast, the ML detector embarks on a comprehensive global search across all transmitting antennas of all users to pinpoint the optimal solution, resulting in significantly higher computational complexity. The LR-RTS detector, as proposed,

TABLE 3. Comparative analysis of computational complexities among various detection techniques.

MUD	Process	Complexity of the algorithm	Complexity Costs		
			4-QAM	16-QAM	64-QAM
ZF	Multiplications	$4N_TN_R(4N_T+1)$	3.361×10^7	3.361×10^7	3.361×10^7
	Additions	$2N_T(8N_TN_R-2N_T-1)$	3.348×10^7	3.348×10^7	3.348×10^7
LR–ZF	Multiplications	$4\,N_TN_R\,(4N_T+1)+K(4\,M_T^2+4M_TN_R)$	3.36×10^7	3.36×10^7	3.36×10^7
	Additions	$2N_T(8N_TN_R-2N_T-1)+K(4\,M_T^2+M_TN_R-2M_T-N_R)$	1.683×10^8	3.355×10^7	3.355×10^7
ZF–LAS	Multiplications	$4N_TN_R(4N_T+1)+4LN_TN_R(2N_T+1)$	5.480×10^7	3.031×10^8	1.111×10^9
	Additions	$2N_T(8N_TN_R-2N_T-1)+4LN_T(4N_TN_R+2N_T-1)$	8.427×10^7	5.724×10^9	6.794×10^{11}
Proposed LR–RTS	Multiplications	$4N_TN_R(4N_T+1)+8LMN_TN_R(2N_T+1)$	4.378×10^8	8.118×10^9	1.358×10^{11}
	Additions	$2N_T(8N_TN_R-2N_T-1)+8LMN_T(4N_TN_R+2N_T-1)$	8.419×10^8	1.620×10^{10}	1.358×10^{11}
ML	Multiplications	$2\,L^{2N_T}\,N_R(2N_T+1)$	8.82×10^{158}	1.182×10^{313}	1.585×10^{467}

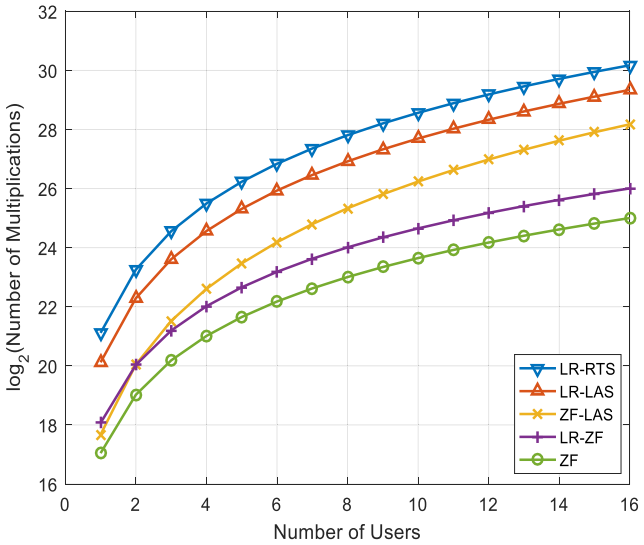

FIGURE 7. Complexity comparison among LR-RTS and classical techniques.

operates with a more extensive search space across all transmitting antennas for each user, aiming to uncover nearly optimal solutions. Consequently, the computational complexity of the LR-RTS detector falls somewhere in between ZF-LAS and ML. It successfully balances computational efficiency and performance, enabling it to approach near-optimal levels of performance with only a slight increase in complexity.

Additionally, Fig. 7 delves into the complexity pertaining to the quantity of multiplications, particularly as the number of users increases. In Fig. 7, we compare the computational complexity of the LR-RTS technique to that of traditional detectors, encompassing ZF, LR-ZF, ZF-LAS, and LR-LAS. This comparative analysis shows that the LR-RTS technique exhibits a slightly higher level of complexity than conventional detectors. However, it is crucial to underscore that this increase in complexity remains marginal, especially when juxtaposed with the significantly elevated computational demands of the ML detector, a point underscored both in Fig. 7 and Table 3. Hence, the additional computational complexity incurred by the LR-RTS technique is fully justified by its capacity to achieve performance levels nearing the ideal standard. Both LAS and RTS are low-complexity signal detection algorithms utilized in Massive MIMO systems, each offering unique approaches and trade-offs. LAS aims to converge to a local maximum of the likelihood function, whereas RTS explores a larger neighborhood, potentially reaching a global maximum closer to the true signal. Consequently, RTS generally exhibits superior BER performance, as evidenced in Fig. 3, although at the expense of increased complexity, as depicted in Fig. 7. Conversely, LAS explores a smaller neighborhood, resulting in significantly lower complexity compared to RTS, rendering it suitable for resource-constrained applications. However, it's worth noting that RTS's complexity is substantially lower than that of the ML detector, as illustrated in Table 2 and Table 3.

The space complexity of the LR-RTS algorithm primarily depends on the storage requirements for lattice basis matrices and the data structures used in the Tabu search. The lattice reduction process requires storing the lattice basis matrix, which has dimensions proportional to the number of antennas and users in the MU-MIMO system. Specifically, for an $(N_R \times N_T)$ MU-MIMO system, the space complexity for storing the lattice basis matrix is $O(N_R \times N_T)$. The RTS algorithm involves maintaining a list of previously visited solutions (Tabu list) to avoid cycles and improve search efficiency. The size of this list affects the space complexity. Typically, the Tabu list size is a small fraction of the search space, resulting in a manageable space complexity. The additional storage for Tabu search operations, such as candidate solutions and search heuristics, adds an overhead of $O(k)$, where k is the maximum number of repetitions allowed in RTS. Combining these factors, the overall space complexity of the

LR-RTS algorithm can be expressed as $O(N_R \times N_T) + O(k)$. Since k is generally much smaller than $(N_R \times N_T)$, the dominant term is $O(N_R \times N_T)$. Thus, the space complexity of the LR-RTS algorithm is primarily determined by the need to store the lattice basis matrices, making it $O(N_R \times N_T)$. This ensures that the algorithm remains efficient and scalable for large-scale MU-MIMO systems, balancing performance with practical memory usage.

VII. CONCLUSION

Our study has presented a novel and promising solution for enhancing the performance of large-scale MU-MIMO systems, specifically addressing the challenge of maintaining reliable communication in large-scale setups. Our research focuses on developing and evaluating the LR-RTS algorithm, which serves as a low-complexity detection technique for these complex and high-capacity wireless systems. Our research findings demonstrate that LR-RTS achieves near-optimal solutions by leveraging lattice reduction and Tabu search-based optimization while maintaining a significantly reduced computational complexity compared to traditional approaches. We have shown that LR-RTS starts with a sound initial solution, LR-ZF, to provide a foundation of accuracy. It guarantees equal or greater accuracy than conventional methods like ZF-LAS and LR-LAS. Notably, the resulting BER is significantly lower with LR-RTS, making it a compelling choice for MU-MIMO systems. Furthermore, the proposed LR-RTS algorithm balances near-optimal performance and manageable computational demands, which is particularly crucial in large-scale MU-MIMO scenarios. In the ever-evolving landscape of wireless communication, LR-RTS represents a breakthrough in enhancing the capabilities of Massive MIMO systems, offering the potential to meet the growing demands of high-performance and large-scale communication networks.

REFERENCES

[1] M. Agiwal, A. Roy, and N. Saxena, "Next generation 5G wireless networks: A comprehensive survey," *IEEE Commun. Surveys Tuts.*, vol. 18, no. 3, pp. 1617–1655, 3rd Quart., 2016, doi: 10.1109/COMST.2016.2532458.

[2] A. Bazzi and M. Chafii, "Secure full duplex integrated sensing and communications," *IEEE Trans. Inf. Forensics Security*, vol. 19, pp. 2082–2097, 2024, doi: 10.1109/TIFS.2023.3346696.

[3] Y. Zhang, J. Du, Y. Chen, X. Li, K. M. Rabie, and R. Kharel, "Near-optimal design for hybrid beamforming in mmWave massive multi-user MIMO systems," *IEEE Access*, vol. 8, pp. 129153–129168, 2020, doi: 10.1109/ACCESS.2020.3009238.

[4] Y. Zhang, J. Du, Y. Chen, X. Li, K. M. Rabie, and R. Khkrel, "Dual-iterative hybrid beamforming design for millimeter-wave massive multi-user MIMO systems with sub-connected structure," *IEEE Trans. Veh. Technol.*, vol. 69, no. 11, pp. 13482–13496, Nov. 2020, doi: 10.1109/TVT.2020.3029080.

[5] Y. He, Y. Chen, Y. Hu, and B. Zeng, "WiFi vision: Sensing, recognition, and detection with commodity MIMO-OFDM WiFi," *IEEE Internet Things J.*, vol. 7, no. 9, pp. 8296–8317, Sep. 2020, doi: 10.1109/JIOT.2020.2989426.

[6] N. Panwar, S. Sharma, and A. K. Singh, "A survey on 5G: The next generation of mobile communication," *Phys. Commun.*, vol. 18, pp. 64–84, Mar. 2016, doi: 10.1016/j.phycom.2015.10.006.

[7] H. Yu, B. Shim, and T. W. Oh, "Iterative interstream interference cancellation for MIMO HSPA+ system," *J. Commun. Netw.*, vol. 14, no. 3, pp. 273–279, Jun. 2012.

[8] T. Zhou, C. Tao, and L. Liu, "LTE-assisted multi-link MIMO channel characterization for high-speed train communication systems," *IEEE Trans. Veh. Technol.*, vol. 68, no. 3, pp. 2044–2051, Mar. 2019, doi: 10.1109/TVT.2018.2875526.

[9] J.-S. Liu, C. R. Lin, and Y.-C. Hu, "Joint resource allocation, user association, and power control for 5G LTE-based heterogeneous networks," *IEEE Access*, vol. 8, pp. 122654–122672, 2020, doi: 10.1109/ACCESS.2020.3007193.

[10] E. Björnson, L. Sanguinetti, H. Wymeersch, J. Hoydis, and T. L. Marzetta, "Massive MIMO is a reality-what is next?: Five promising research directions for antenna arrays," *Digit. Signal Process.*, vol. 94, pp. 3–20, Nov. 2019.

[11] J. Zhang, E. Björnson, M. Matthaiou, D. W. K. Ng, H. Yang, and D. J. Love, "Prospective multiple antenna technologies for beyond 5G," *IEEE J. Sel. Areas Commun.*, vol. 38, no. 8, pp. 1637–1660, Aug. 2020.

[12] J. Navarro-Ortiz, P. Romero-Diaz, S. Sendra, P. Ameigeiras, J. J. Ramos-Munoz, and J. M. Lopez-Soler, "A survey on 5G usage scenarios and traffic models," *IEEE Commun. Surveys Tuts.*, vol. 22, no. 2, pp. 905–929, 2nd Quart., 2020, doi: 10.1109/COMST.2020.2971781.

[13] X. Chen, D. W. K. Ng, W. Yu, E. G. Larsson, N. Al-Dhahir, and R. Schober, "Massive access for 5G and beyond," *IEEE J. Sel. Areas Commun.*, vol. 39, no. 3, pp. 615–637, Mar. 2021, doi: 10.1109/JSAC.2020.3019724.

[14] U. V. Menon, N. R. Challa, and K. Bagadi, "Lenstra lenstra Lovász (LLL) assisted likelihood ascent search (LAS) algorithm for signal detection in massive MIMO," in *Proc. Int. Conf. Vis. Towards Emerg. Trends Commun. Netw. (ViTECoN)*, Vellore, India, Mar. 2019, pp. 1–4, doi: 10.1109/ViTECoN.2019.8899594.

[15] A. Morgado, K. M. S. Huq, S. Mumtaz, and J. Rodriguez, "A survey of 5G technologies: Regulatory, standardization and industrial perspectives," *Digit. Commun. Netw.*, vol. 4, no. 2, pp. 87–97, Apr. 2018, doi: 10.1016/j.dcan.2017.09.010.

[16] N. R. Challa and K. Bagadi, "Design of massive multiuser MIMO system to mitigate inter antenna interference and multiuser interference in 5G wireless networks," *J. Commun.*, vol. 15, no. 9, pp. 693–701, Sep. 2020, doi: 10.12720/jcm.15.9.693-701.

[17] N. Fatema, G. Hua, Y. Xiang, D. Peng, and I. Natgunanathan, "Massive MIMO linear precoding: A survey," *IEEE Syst. J.*, vol. 12, no. 4, pp. 3920–3931, Dec. 2018, doi: 10.1109/JSYST.2017.2776401.

[18] K. Zhi, C. Pan, H. Ren, and K. Wang, "Ergodic rate analysis of reconfigurable intelligent surface-aided massive MIMO systems with ZF detectors," *IEEE Commun. Lett.*, vol. 26, no. 2, pp. 264–268, Feb. 2022, doi: 10.1109/LCOMM.2021.3128904.

[19] K. M. Rege, K. Balachandran, J. H. Kang, and M. Kemal Karakayali, "Practical dirty paper coding with sum codes," *IEEE Trans. Commun.*, vol. 64, no. 2, pp. 441–455, Feb. 2016, doi: 10.1109/TCOMM.2015.2499278.

[20] T. Özcan and A. M. Y. Turgut, "Constant envelope precoding and non-orthogonal multiple access for massive MIMO systems," in *Proc. 28th Signal Process. Commun. Appl. Conf. (SIU)*, Gaziantep, Turkey, Oct. 2020, pp. 1–4, doi: 10.1109/SIU49456.2020.9302057.

[21] A. R. Flores, R. C. De Lamare, and B. Clerckx, "Tomlinson-harashima precoded rate-splitting with stream combiners for MU-MIMO systems," *IEEE Trans. Commun.*, vol. 69, no. 6, pp. 3833–3845, Jun. 2021, doi: 10.1109/TCOMM.2021.3065145.

[22] S. Lyu and C. Ling, "Hybrid vector perturbation precoding: The blessing of approximate message passing," *IEEE Trans. Signal Process.*, vol. 67, no. 1, pp. 178–193, Jan. 1, 2019, doi: 10.1109/TSP.2018.2877205.

[23] H. Semira, F. Kara, H. Kaya, and H. Yanikomeroglu, "Multi-user joint maximum-likelihood detection in uplink NOMA-IoT networks: Removing the error floor," *IEEE Wireless Commun. Lett.*, vol. 10, no. 11, pp. 2459–2463, Nov. 2021, doi: 10.1109/LWC.2021.3103937.

[24] A. H. Sawalmeh, N. S. Othman, H. Shakhatreh, and A. Khreishah, "Wireless coverage for mobile users in dynamic environments using UAV," *IEEE Access*, vol. 7, pp. 126376–126390, 2019, doi: 10.1109/ACCESS.2019.2938272.

[25] N. R. Challa and K. Bagadi, "Lattice reduction assisted likelihood ascent search algorithm for multiuser detection in massive MIMO system," in *Proc. 15th IEEE India Council Int. Conf. (INDICON)*, Coimbatore, India, Dec. 2018, pp. 1–5, doi: 10.1109/INDICON45594.2018.8987139.

[26] C.-E. Chen and W.-H. Sheen, "Design of lattice reduction algorithms for linear-precoded MIMO system," *IEEE Wireless Commun. Lett.*, vol. 3, no. 1, pp. 46–49, Feb. 2014, doi: 10.1109/WCL.2013.110713.130693.

[27] J. Park, B. Clerckx, J. Chun, and B. J. Jeong, "Lattice reduction-aided successive interference cancelation for MIMO interference channels," *IEEE Trans. Veh. Technol.*, vol. 63, no. 8, pp. 4131–4135, Oct. 2014, doi: 10.1109/TVT.2014.2302323.

[28] N. R. Challa and K. Bagadi, "Likelihood ascent search detection for coded massive MU-MIMO systems to mitigate IAI and MUI," *Radioelectronics Commun. Syst.*, vol. 63, no. 5, pp. 223–234, May 2020, doi: 10.3103/s0735272720050015.

[29] D. C. Araujo, T. Maksymyuk, A. L. F. Almeida, T. Maciel, J. C. M. Mota, and M. Jo, "Massive MIMO: Survey and future research topics," *IET Commun.*, vol. 10, no. 15, pp. 1938–1946, Oct. 2016, doi: 10.1049/iet-com.2015.1091.

[30] Y. Ge, W. Zhang, F. Gao, and G. Y. Li, "Frequency synchronization for uplink massive MIMO with adaptive MUI suppression in angle domain," *IEEE Trans. Signal Process.*, vol. 67, no. 8, pp. 2143–2158, Apr. 2019, doi: 10.1109/TSP.2019.2901344.

[31] J. Zeng, Q. Xu, X. Fan, N. Ye, W. Ni, and Y. J. Guo, "Achieving URLLC by MU-MIMO with imperfect CSI: Under k–μ shadowed fading," *IEEE Wireless Commun. Lett.*, vol. 11, no. 12, pp. 2560–2564, Dec. 2022.

[32] M. Sakai, K. Kamohara, H. Iura, H. Nishimoto, K. Ishioka, Y. Murata, M. Yamamoto, A. Okazaki, N. Nonaka, S. Suyama, J. Mashino, A. Okamura, and Y. Okumura, "Experimental field trials on MU-MIMO transmissions for high SHF wide-band massive MIMO in 5G," *IEEE Trans. Wireless Commun.*, vol. 19, no. 4, pp. 2196–2207, Apr. 2020, doi: 10.1109/TWC.2019.2962766.

[33] Y. Xia, C. Jayawardena, and K. Nikitopoulos, "Reduced complexity matrix inversions in slow time-varying MIMO channels," in *Proc. IEEE Int. Conf. Commun.*, May 2022, pp. 456–461, doi: 10.1109/ICC45855.2022.9838292.

[34] H. Wang, Y. Ji, Y. Shen, W. Song, M. Li, X. You, and C. Zhang, "An efficient detector for massive MIMO based on improved matrix partition," *IEEE Trans. Signal Process.*, vol. 69, pp. 2971–2986, 2021, doi: 10.1109/TSP.2021.3064781.

[35] P. V. Amadori and C. Masouros, "Interference-driven antenna selection for massive multiuser MIMO," *IEEE Trans. Veh. Technol.*, vol. 65, no. 8, pp. 5944–5958, Aug. 2016, doi: 10.1109/TVT.2015.2477457.

[36] M. Yuan, H. Wang, and Y. Sun, "BD-UCD-Based nonlinear hybrid precoding for millimeter wave massive multiuser MIMO systems," *IEEE Commun. Lett.*, vol. 25, no. 3, pp. 1010–1014, Mar. 2021, doi: 10.1109/LCOMM.2020.3034131.

[37] J. Liao, J. Zhao, F. Gao, and G. Y. Li, "Deep learning aided low complex sphere decoding for MIMO detection," *IEEE Trans. Commun.*, vol. 70, no. 12, pp. 8046–8059, Dec. 2022, doi: 10.1109/TCOMM.2022.3218630.

[38] H. C. Nguyen, E. de Carvalho, and R. Prasad, "Multi-user interference cancellation schemes for carrier frequency offset compensation in uplink OFDMA," *IEEE Trans. Wireless Commun.*, vol. 13, no. 3, pp. 1164–1171, Mar. 2014, doi: 10.1109/TWC.2014.021414.070718.

[39] H. C. Nguyen, E. de Carvalho, and R. Prasad, "Multi-user interference cancellation scheme(s) for muliple carrier frequency offset compensation in uplink OFDMA," in *Proc. IEEE 17th Int. Symp. Pers., Indoor Mobile Radio Commun.*, Helsinki, Finland, Sep. 2006, pp. 1–5, doi: 10.1109/PIMRC.2006.254335.

[40] A. Bazzi and M. Chafii, "On integrated sensing and communication waveforms with tunable PAPR," *IEEE Trans. Wireless Commun.*, vol. 22, no. 11, pp. 7345–7360, Nov. 2023, doi: 10.1109/TWC.2023.3250263.

[41] A. K. Sah and A. K. Chaturvedi, "Sequential and global likelihood ascent search-based detection in large MIMO systems," *IEEE Trans. Commun.*, vol. 66, no. 2, pp. 713–725, Feb. 2018, doi: 10.1109/TCOMM.2017.2761383.

[42] N. R. Challa and K. Bagadi, "Design of near-optimal local likelihood search-based detection algorithm for coded large-scale MU-MIMO system," *Int. J. Commun. Syst.*, vol. 33, no. 12, pp. 1–12, Apr. 2020, doi: 10.1002/dac.4436.

[43] N. R. Challa and K. Bagadi, "Design of large scale MU-MIMO system with joint precoding and detection schemes for beyond 5G wireless networks," *Wireless Pers. Commun.*, vol. 121, no. 3, pp. 1627–1646, Jul. 2021, doi: 10.1007/s11277-021-08688-6.

[44] K. Bagadi, C. V. Ravikumar, M. Alibakhshikenari, N. Challa, A. Rajesh, S. Aïssa, I. Dayoub, F. Falcone, and E. Limiti, "Precoded large scale multi-user-MIMO system using likelihood ascent search for signal detection," *Radio Sci.*, vol. 57, no. 12, pp. 1–12, Dec. 2022, doi: 10.1029/2022RS007573.

[45] S. Chakraborty, N. B. Sinha, and M. Mitra, "Low complexity hybrid layered tabu-likelihood ascent search for large MIMO detection with perfect and estimated channel state information," *ETRI J.*, vol. 45, no. 3, pp. 418–432, Jun. 2023, doi: 10.4218/etrij.2022-0052.

[46] A. K. Sah and A. K. Chaturvedi, "An unconstrained likelihood ascent based detection algorithm for large MIMO systems," *IEEE Trans. Wireless Commun.*, vol. 16, no. 4, pp. 2262–2273, Apr. 2017, doi: 10.1109/TWC.2017.2661283.

[47] Y. Han, S. Jin, M. Matthaiou, T. Q. S. Quek, and C.-K. Wen, "Towards extra large-scale MIMO: New channel properties and low-cost designs," *IEEE Internet Things J.*, vol. 10, no. 16, pp. 14569–14594, Aug. 2023, doi: 10.1109/JIOT.2023.3273328.

KALAPRAVEEN BAGADI (Senior Member, IEEE) received the B.E. degree in electronics and communication engineering from Andhra University, India, in 2006, and the M.Tech. degree in electronic systems and communication and the Ph.D. degree in wireless communication from the Department of Electrical Engineering, National Institute of Technology, Rourkela, India, in 2009 and 2014, respectively. He was a Full Professor with the School of Electronics Engineering (SENSE), Vellore Institute of Technology (VIT), Vellore, India, until April 2023. Currently, he is with the School of Electronics Engineering (SENSE), VIT-AP University, Amaravati, Andhra Pradesh, India. He has guided six Ph.D. theses and is currently guiding three scholars. He has published over 65 research articles in various refereed international journals, such as IEEE Access, *Neural Computing and Applications*, *Wireless Personal Communications*, *IET Communication*, *International Journal of Communication Systems*, and *Radio Science*. His research interests include SDMA, MIMO, OFDM, NOMA, D2D communication, cognitive radio, UAV communication, and artificial intelligence. He reviews a journals, such as IEEE Access, *Wireless Personal Communications*, *IET Communications*, and *Telecommunication Systems*. He is an Academic Editor of *Wireless Communication and Mobile Computing* and *Applied Computational Intelligence and Soft Computing*.

VISALAKSHI ANNEPU received the B.Tech. degree in computer science and engineering from Jawaharlal Nehru Technical University, Kakinada, India, in 2011, the M.Tech. degree in computer science and Technology from Andhra University, Visakhapatnam, India, in 2013, and the Ph.D. degree in computer networks from VIT, Vellore, India, in 2020. She was an Assistant Professor with the Department of Computer Engineering, Sri Sivani Institute of Technology, Srikakulam, Andhra Pradesh, from June 2014 to May 2016. Currently, she is an Assistant Professor with the School of Computer Science and Engineering, VIT-AP University, Amaravati, India. Her research interests include wireless networking, artificial intelligence, soft computing techniques, and neural networks.

NAGA RAJU CHALLA received the B.Tech. degree in electronics engineering from the Prasad V. Potluri Siddhartha Institute of Technology, Vijayawada, Andhra Pradesh, India, in 2009, the M.E. degree in embedded systems from Sathyabama University, Chennai, in 2012, and the Ph.D. degree in wireless communication from Vellore Institute of Technology, Vellore, in 2021. Currently, he is an Assistant Professor with the Department of Electronics and Communication Engineering, Bapatla Engineering College, Bapatla, Andhra Pradesh. He has published several research articles in various journals. His main research interests include massive MU-MIMO, wireless communication, 5G and 6G wireless communication systems, deep learning/machine learning communication systems, AI-based systems, and tera heartz communication systems. He is a Reviewer of *Wireless Personal Communications*, *IET Communications*, IEEE TRANSACTIONS ON VEHICULAR TECHNOLOGY, and IEEE SENSORS JOURNAL.

FRANCESCO BENEDETTO (Senior Member, IEEE) has been the Chair of the IEEE 1900.1 Standard "Definitions and Concepts for Dynamic Spectrum Access: Terminology Relating to Emerging Wireless Networks, System Functionality, and Spectrum Management," since 2016. He has been the Leader of the WP 3.5 on "Development of Advanced GPR Data Processing Technique" of the European COST Action TU1208—Civil Engineering Applications of Ground Penetrating Radar. He is the General Co-Chair of the IEEE 43rd International Conference on Telecommunications and Signal Processing (TSP 2020), the General Chair of the Series of International Workshops on Signal Processing for Secure Communications (SP4SC 2014, 2015, and 2016), and the Lead Guest Editor of the Special Issue on "Advanced Ground Penetrating Radar Signal Processing Techniques" for the *Signal Processing* journal (Elsevier). He is a TPC member of several IEEE international conferences and symposia. He served as a reviewer for several IEEE TRANSACTIONS, IET Proceedings, EURASIP, and Elsevier journals. He is an Associate Editor of IEEE ACCESS, an Editor of the IEEE SDN Newsletter, an Associate Editor of the *AEÜ–International Journal of Electronics and Communications* (Elsevier), and the Editor-in-Chief of the international journal *Recent Advances on Computer Science and Communications* (Bentham).

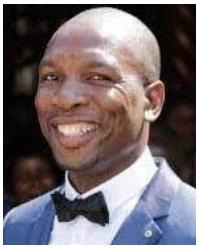

THOKOZANI SHONGWE (Senior Member, IEEE) received the B.Eng. degree in electronic engineering from the University of Swaziland, Swaziland, in 2004, the M.Eng. degree in telecommunications engineering from the University of the Witwatersrand, South Africa, in 2006, and the D.Eng. degree from the University of Johannesburg, South Africa, in 2014. He is currently an Associate Professor with the Department of Electrical and Electronic Engineering Technology, University of Johannesburg. His research interests include communications, error-correcting coding, power-line communications, cognitive radio, smart grids, visible light communications, machine learning, and artificial intelligence. He was a recipient of the 2014 University of Johannesburg Global Excellence Stature (GES) Award, which was awarded to him to carry out his postdoctoral research with the University of Johannesburg. He was also a recipient of the TWAS-DFG Cooperation Visits Program funding to carry out research in Germany, in 2016. He also received the Post-Graduate Merit Award Scholarship to pursue the master's degree with the University of the Witwatersrand, in 2005, which was awarded on a merit basis. In 2012, he (and his co-authors) received the Best Student Paper Award from the IEEE ISPLC 2012 (Power Line Communications Conference), Beijing, China.

KHALED RABIE (Senior Member, IEEE) received the M.Sc. and Ph.D. degrees in electrical and electronic engineering from The University of Manchester, in 2011 and 2015, respectively. He is currently a Reader with the Department of Engineering, Manchester Metropolitan University (MMU), U.K. He has worked as a part of several largescale industrial projects and has published more than 200 journals and conference papers (mostly IEEE). His current research interest includes designing and developing next-generation wireless communication systems. He is a fellow of the U.K. Higher Education Academy (FHEA) and the European Alliance for Innovation (EAI). He has received many awards over the past few years in recognition of his research contributions, including the Best Paper Awards at the 2021 IEEE CITS and the 2015 IEEE ISPLC and IEEE ACCESS Editor of the Month Award for August 2019. He serves regularly on the Technical Program Committee (TPC) for several major IEEE conferences, such as GLOBECOM, ICC, and VTC. He is currently serving as an Editor for IEEE COMMUNICATIONS LETTERS and *IEEE Internet of Things Magazine*.